

A unique mechanism of nuclear division in *Giardia lamblia* involves components of the ventral disk and the nuclear envelope

ALBERTO J. SOLARI*, MONICA I. RAHN*, ALICIA SAURA**, AND HUGO D. LUJAN**

* Centro de Investigaciones en Reproduccion, Facultad de Medicina, UBA, Buenos Aires, Argentina.

** Catedra de Bioquímica y Biología Molecular, Facultad de Medicina, Universidad Nacional de Córdoba, Córdoba, Argentina

Key words: *Giardia*, primitive mitosis, fine structure of mitosis, protist mitosis, cell differentiation

ABSTRACT: The fine structure of the binucleate, parasitic protist *Giardia lamblia* during interphase and divisional stages was studied by serial thin sectioning and three-dimensional reconstructions. The earlier sign of nuclear division is the development of a few peripheral areas of densely packed chromatin directly attached to the inner nuclear envelope. An intracytoplasmic sheet of ventral disk components grows from the cell periphery towards one of the nuclei, apparently constricting this nucleus, which becomes located at a ventral bulge. After the basal bodies become duplicated, a full nuclear division occurs in trophozoites, giving two pairs of parent-daughter nuclei. This full division occurs in a dorsal-ventral direction, with the resulting nuclear pairs located at the sides of the two sets of basal bodies. A new ventral disk is formed from the disk-derived sheets in the cell harboring the four nuclei. Cytokinesis is polymorphic, but at early stages is dorsal-to-dorsal. Encysting trophozoites show the development of Golgi cisternae stacks and dense, specific secretory granules. 3-D reconstructions show that cysts contain a single pair of incompletely strangled nuclei. The dividing *Giardia* lacks a typical, microtubular spindle either inside or outside the nuclei. The nuclear envelope seems to be the only structure involved in the final division of the parent-daughter nuclei.

Introduction

Giardia lamblia is an intestinal parasite of humans and other vertebrates that belongs to the earliest diverging branches of the eukaryotic lineage of descent. *Giardia* infections are initiated with the ingestion of cysts, followed by their excystation and colonization of the small intestine by the trophozoites (Adam, 2001). To survive outside the host's intestine, trophozoites differentiate (encyst) into infective cysts, which are excreted in the feces and responsible for the transmission of the disease among susceptible hosts (Lujan *et al.*, 1998).

The ultrastructural features and molecular mechanisms of cell division of this binucleate protozoan are presently unknown (Nohynkova *et al.*, 2000) and the

morphology of its cytokinesis has been judged as uncertain (reviewed by Adam, 2001). Despite the lack of these basic data, this protist, which belongs to the class Diplomonadea, Mastigophora (Harrison and Corliss, 1991), is presently under intensive research from the viewpoints of its biochemistry (reviewed in Adam, 2001), the encystation processes (Lujan *et al.*, 1995a and b; Lujan *et al.*, 1997), its phylogenetic status (Roger *et al.*, 1999) and its genome, which is largely (90-95%) sequenced (Adam, 2001; Yu *et al.*, 2002; see also the *Giardia* genome project site in Internet: <http://jbpc.mbl.edu/Giardia>). The haploid DNA content of *G. lamblia* is considered to be 12 Mb as the added DNA content of the five "chromosomes" seen in electrokaryotypes by pulsed-field gel electrophoresis adds to this amount (Adam, 2001; Le Blancq and Adam, 1998). However, the total DNA of this binucleate protist gives about 1.3×10^8 bp (Yu *et al.*, 2002) and thus each of the two nuclei is considered polyploid, with a suggested ploidy of four (Yu *et al.*, 2002). The nuclear division of

Address correspondence to: Dr. Alberto Solari. CIR, Facultad de Medicina, Paraguay 2155, (1121) Buenos Aires, ARGENTINA. Fax/Phone: (54-11) 4961 2763; E-mail: asolari@fmed.uba.ar
Received on February 14, 2003. Accepted on May 30, 2003

a polyploid, asexual protozoan as *G. lamblia* is of considerable interest to investigate the evolution of mitotic mechanisms among lower eukaryotes. Additionally, since *Giardia* differentiation (encystation/excystation) has been linked to cell division events, it is important to know how the life and cell cycle of this protist are related in order to understand fundamental cellular processes occurring during differentiation, such as the expression of specific genes and the biogenesis of secretory organelles (Lujan *et al.*, 1997, 1998).

Some recent papers have dealt with the subject of the nuclear symmetry at the division process (Ghosh *et al.*, 2001; Yu *et al.*, 2002) and both studies agree that the nuclei are equationally partitioned at cytokinesis, although they disagree as regards to either ventral:ventral or dorsal:ventral cytokinesis. In addition, light-microscopy has not explained the mechanisms of cell division in this protist, despite detailed descriptions of its nuclear morphology (Filice, 1952).

Thus, this work was aimed to show the fine structural features of nuclear and cytoplasmic organelles related to cell division during the different stages of the *Giardia*'s life-cycle in order to provide new insights into the molecular events controlling these mechanisms. Here we demonstrate that trophozoites show two features in their divisional behavior: (a) The "downwards type" of nuclear constriction, which occurs either in vegetative trophozoites or in trophozoites undergoing encystation, in which one of the nuclei becomes strangled and moves towards the ventral cup-like surface forming a large ball that may initiate cyst formation, and (b) A second feature of division in non-encysting trophozoites, which is the complete separation of two pairs of daughter nuclei. This full division type may occur also at the excysting stage, but with some differences as regards to cytokinesis. Previously proposed, contradictory hypotheses on the mechanism of cell division in *Giardia* have shown the need of further structural investigations through the life cycle of this protist.

Materials and Methods

Source and cultivation

Trophozoites of the isolates C6 (Nash, 1992) were cultured in TYI-S-33 medium supplemented with 10% adult bovine serum and 0.5 mg/ml bovine bile (growth medium) as described (Diamond *et al.*, 1978). Encystation of trophozoite monolayers was accomplished by

the method described by Boucher and Gillin (1990). Briefly, vegetative trophozoites were cultured for 72 h in either 15 ml borosilicate glass tubes or 25 ml culture flask containing growth medium without bovine bile (pre-encystation medium). The medium was then decanted and encystation medium (pre-encystation medium plus porcine bile and lactic acid at pH 7.8) was added to the tubes. After 48 h, cysts were collected from the culture supernatant and adhered cells (encysting trophozoites) harvested and processed as described below.

Electron microscopy

Cultures were fixed *in situ* to preserve the cell organization when attached to the wall of the culture flask. After the first 30 min in fixative, the flask wall was lightly scraped to detach the trophozoites, the resulting suspension was centrifuged at 500 g, and the pellet placed in fresh fixative for the completion of fixation. Two main different fixatives were used: 2.5% glutaraldehyde in 0.1 M sodium cacodylate buffer, pH 7.1; or alternatively, Karnovsky's fixative (2% formaldehyde prepared from paraformaldehyde, plus 1% glutaraldehyde in either 0.1 M cacodylate buffer or 0.1 M phosphate buffer, pH 7.0). It was found that temperature of fixation was critical for preservation. The best results come from fixation at 37°C or at room temperature. Protists fixed after a 15 min cold treatment at 4°C showed poor preservation of cytoplasmic and nuclear structures. Fixation was performed for 2 to 24 h, and it was followed by postfixation in 1% Os O4 for 1-2 h, with the addition of 1.25% potassium ferrocyanide. During dehydration, the tissue was pre-stained with 1% uranyl acetate in 70% ethanol for 2 h. The pellets were embedded in araldite and sections were cut in a Porter-Blum ultramicrotome as series of attached sections in order to provide the data for 3-dimensional reconstructions. Two types of serial sections were used: Thin, silver interference color (about 60 nm in thickness) were the ones used routinely; and eventually, 250 nm thick sections were used for rapid screening of *Giardia* life-cycle stages. Single whole grids (oval, 2 mm x 1 mm, Pelco International, Redding, CA) were always used for collecting segments of 20 sections from series of 100-120 thin sections. The sections were stained first with saturated uranyl-acetate in water and then with lead citrate. Sections were examined in a Siemens Elmiskop at magnifications standardized with diffraction grids. Series of micrographs taken at the same magnification were enlarged as positives, and each positive was digitized in a Hewlett-Packard Scanjet 3400C scanner. The

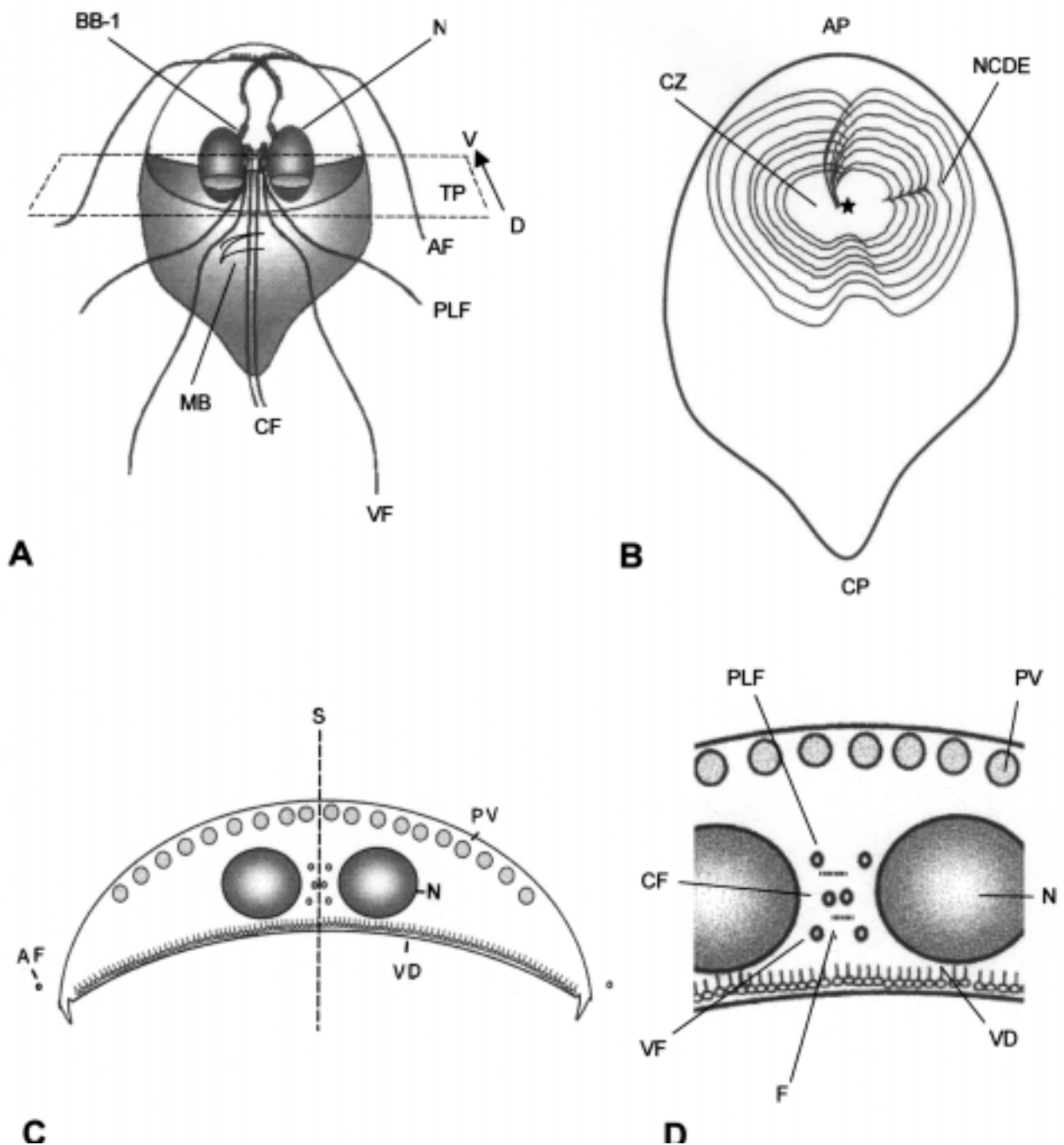


FIGURE 1 A-D. Schematic drawings of the structure of vegetative trophozoites of *G. lamblia*. A: General view in the frontal plane (dorsal view). N: nucleus. AF, PLF, VF and CF respectively, anterior, postero-lateral, ventral and caudal flagella. MB: medium body. BB1: basal body of anterior flagella. The transverse plane (TP) and the perspective of dorsal (D) to ventral (V) sides is marked by the arrow. B: ventral view of the frontal plane, in which the spiral array of ventral disk ridges is shown. AP, CP, anterior and caudal poles. CZ: central zone having no ventral disk. NCDE: nuclear constricting, disk derivative expansion. Star: origin of disk ridges from the opposite, caudal basal body. C: cross-section (in the transverse plane). S: sagittal plane passing between the two caudal flagella. N: nucleus. VD: ventral disk. PV: peripheral vesicles (lysosomes). AF: anterior flagella already outside the cytoplasm. D: detail of the central region in the cross-section. PLF, CF and VF, postero-lateral, caudal and ventral flagella. F: funis (microtubular rows). N: nucleus. PV: peripheral vesicles. VD: ventral disk showing the microtubular row and the cross-sectioned ribbons on the microtubules.

digitized images were processed with the IGL TRACE program for 3-dimensional reconstructions. Profile, slab or surface reconstructions were observed and saved with a GL VIEW 3.0 Viewer operated with a Pentium III PC (500 MHz).

Light microscopy

Smears of spread trophozoites were fixed with either one of two protocols. For morphological observations, pellets of centrifuged cells were fixed with Carnoy's fixative (ethanol: acetic acid, 3:1) for 15 min, refixed with renewal of fixative and then drops of the cell suspension were spread on slides, dried and stained either with Giemsa stain or with a mixture of 50% silver nitrate (2 parts) and 2% gelatin and 1% formic acid (one part) at 40°C (Solari, 1998). For other studies pellets were fixed with 1% formaldehyde (prepared from paraformaldehyde in 0.01 M sodium borate buffer, pH 7.0 for 5 min, washed in 0.4% photoflo (Kodak), and then spread on slides and dried or kept in 100% ethanol at -20°C before study.

Results

1. The vegetative trophozoite

A. General features:

Due to the complexity of its organelles, it is useful to label each of the incidence planes of the sections of *Giardia*: frontal, transverse and sagittal, and their oblique derivatives (Fig. 1A-D). In a frontal plane (Fig. 1A), the overall shape of the trophozoite and its eight flagella are readily identified. The two caudal flagella are straight in their intracytoplasmic region and located just at both sides of the longitudinal axis of the cell. The two nuclei are located in the anterior half of the cell, at the left and right sides of the longitudinal cell axis (Figs. 1A and 2). At the medial sides of both nuclei there are four basal bodies from which stem the flagella corresponding to each of the nucleus (Figs. 1A and 3). The most anterior (cephalic) of these basal bodies are the ones corresponding to the anterior flagella (BB1 in Figs. 1A and 3). The other basal bodies are more central and closer to each other (Fig. 1A). The drawing of Fig. 1A corresponds to a view from the dorsal surface of the trophozoite, which is then sectioned in the transverse plane in Fig. 1C. However, when viewed from the ventral surface (Fig. 1B), the image is different and

shows the cup-shaped, large "ventral disk" at the anterior half of the cell. *Giardia* is generally assumed to have bilateral symmetry (reflective) in the left-right axis. However, as shown by its prominent ventral disk, it has rotational-displacement symmetry, that is a spiral type of symmetry (Figs. 1B and 3). The ventral disk is a cup-like depression, which has spiral symmetry in a clockwise direction when viewed from the ventral side. The disk does not reach the outer and frontal sides of the ventral surface (Fig. 1B) and shows a notch at the caudal side. The outer sides of this ventral surface are formed by a cytoplasmic expansion called "ventro-lateral flange" that is located at the frontal, left and right sides of the edge of the ventral disk (see Fig. 4, VLF). Caudal to the ventral disk, the cytoplasm becomes thinner and expands towards the caudal pole (CP, Fig 1B). The ventral disk shows a central zone (CZ in Fig. 2B), which lacks an underlying cytoskeleton (there are no internal ridges at this zone). This central zone corresponds just to the group of basal bodies in the inner cytoplasm. A series of cytoskeleton structures stem from one of these bodies (star in Fig. 1B and upper arrow in Fig. 3). These cytoskeleton structures form the inner spiral ridges and a special sheet that makes a nuclear constriction ("nuclear constricting derivative expansion", NCDE in Fig. 2B) during the divisional stages.

A cross-section in the transverse plane that crosses the nuclei (N) is shown in Fig. 1C and in Figs. 4 and 5. The crescent shape of the cell is typical, with the ventral disk cytoskeleton (VD in Fig. 1C, and in Figs. 4, 5 and 6) adjacent to the lower concave surface, and the rim of peripheral vesicles (PV in Figs. 1C, 2 and 4) in the upper, convex cytoplasmic region. The sagittal plane (S in Fig. 1C) passes in between the two groups of flagella directed towards the caudal pole. The anterior flagella (AF in Figs. 1A and 1C) are already at the outside and parallel to the sides of the cell in this section. In an enlarged central region (Figs. 1D and 5), the caudal flagella (CF) are recognized as the more medial ones, while the posterolateral (PLF) and ventral flagella (VF) are less medial. Furthermore, the caudal flagella can be recognized by their companion "funis" microtubules that form two small layers alongside the CF (F in Figs. 1D and 5).

B. Fine structure:

The fine structure of the trophozoite agrees with previous reports of the fine structure of this species (Reviewed in Adam, 2001) and the detailed report on the similar one, *Giardia muris* (Friend, 1966). The pro-

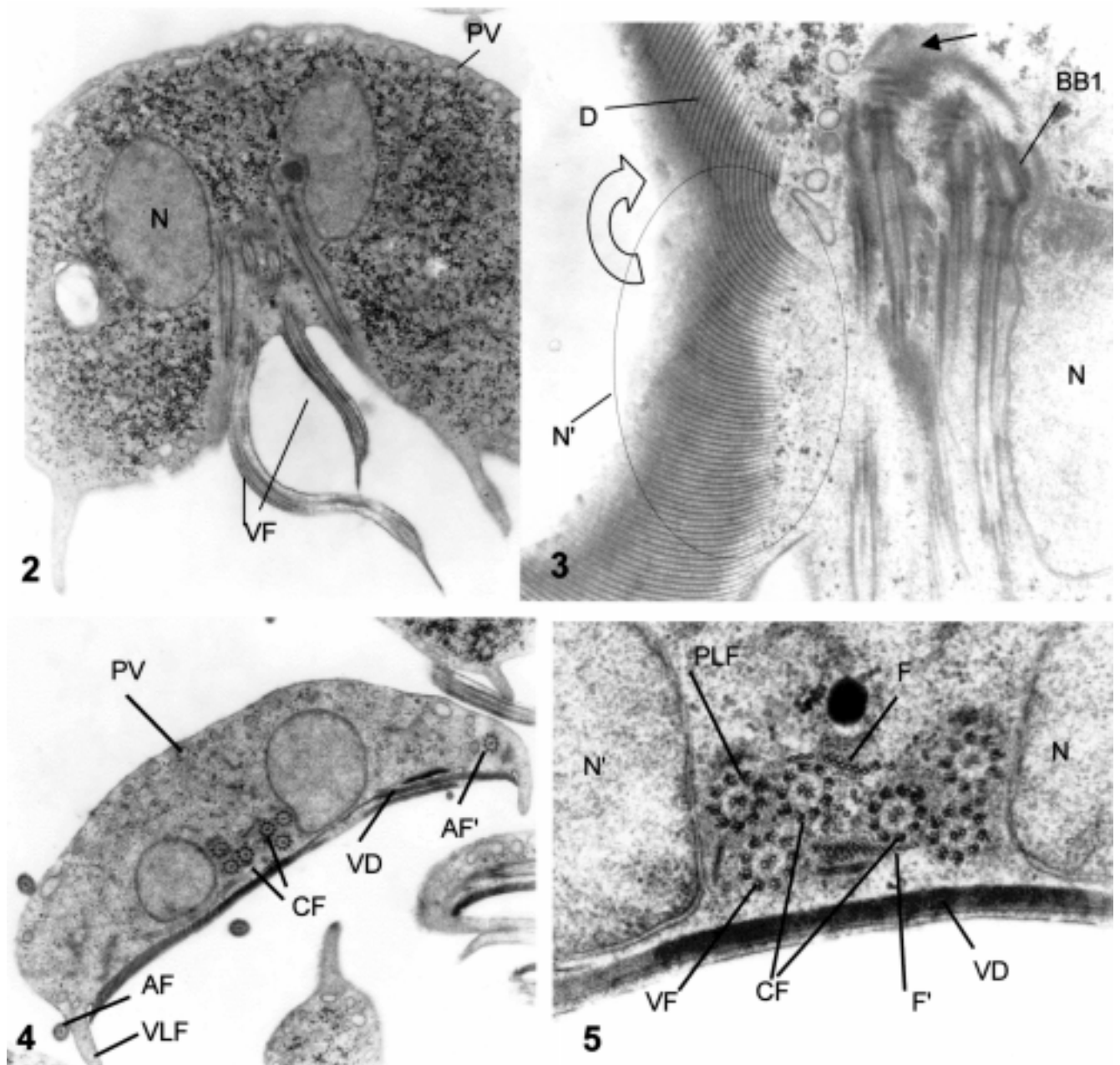


FIGURE 2. Thin section in a frontal view passing through the emergence of the ventral flagella (VF) in a caudal direction. N: nucleus. PV: peripheral vesicles. X 11,000.

FIGURE 3. Thin section in a frontal plane slightly tilted downwards to the left side. On the right side the nucleus (N) is visible. In the left side the plane shows the spiral ventral disk ridges (D and open arrow) and the outline of the left nucleus (N') is marked. BB1: basal body of anterior flagellum. The straight arrow points to the origin of the disk ridges from the horizontal dense rods lying on the anterior pole of a caudal basal body. X 20,000.

FIGURE 4. Thin section in the transverse plane. CF and AF-AF', caudal and anterior flagella. VLF: ventrolateral flange. VD, ventral disk in cross-section. PV: peripheral vesicles. X 10,500

FIGURE 5. Detail of the central, cross-section. N and N', nuclei. PLF, VF and CF, posterolateral, ventral and caudal flagella. VD: the ventral disk, obliquely sectioned near its notch. F and F': the microtubular rows of the "funis", above and below the two caudal flagella. X 48,000

tist has two oval-shaped nuclei, surrounded by a nuclear envelope formed by two membranes and an intermembranous space (Figs. 2 and 5). The central longitudinal axis is the region in which the first segments of the 8 flagella of *Giardia* are located (Fig. 1A and 3). The flagella form two groups of four and each group corresponds to one nucleus. They are classified as: a) anterior (also called anterolateral), b) caudal, c) ventral, and d) posterolateral (see Figs. 1, and 2-5). Their corresponding basal bodies, located towards the anterior end of the nuclei, can be distinguished by their specific locations and peripheral structures. In a frontal view, the overall shape of the trophozoite is pear-like, with the nuclei located towards the anterior side, and six of the eight flagella (those of b, c, and d type) are directed towards the caudal side, while the "anterior" flagella show a curved path inside the cytoplasm. This path is first oriented towards the front, then crosses-over to the opposite side, and emerges laterally from the cytoplasm (drawing in Fig. 1A and micrographs in Fig. 10b-d). In the intracytoplasmic part of the path of these AF, a special paraxial substructure goes along the axonemes. These paraxial structures have a characteristic striation with a regular periodicity in the convex side (Fig. 1A and Fig. 10 c-d), which is different from that observed in the ridges of the ventral disk.

The cytoplasm of the trophozoite has abundant glycogen granules which appear densely stained after ferrocyanide treatment (Fig. 2) and which are homogeneously dispersed throughout the cytoplasm, except at the peripheral rim of vesicles of lysosomal nature (Fig. 2, PV). No Golgi membranous elements can be observed at this stage. On the other hand, there are relatively scarce cisternae with a grayish contents.

The nuclei have at this stage an homogeneous, pale staining (Fig. 2). No nucleolus is apparent at this or any other stage of the cell cycle and life cycle. The chromatin appears as threads thinner than the 25-30 nm wide chromatin fibers usually seen in eukaryotes. The nuclear envelope shows two membranes with very scarce occurrence of nuclear pores at this stage. In fact, the profiles of the two membranes can often be observed uninterrupted in at least half the profile of each nucleus (Fig. 2).

In a cross-section (transverse) central to the trophozoite (Fig. 4), the outlines of the two nuclei remain oval, and the six flagella caudally oriented appear in cross-section (Figs. 4 and 5). The ventral disk (drawing in Fig. 1C and micrograph in Fig. 6) is formed by a single rim of microtubules located immediately below the cell membrane. Each microtubule has a perpendicular fibrous ribbon that appears in these cross-sections

as a dense stalk about 6-10 times the size of the attached microtubule (Fig. 6). These stalks are in fact ribbons as seen in tangential sections (Fig. 3). In-between each pair of microtubule and stalks there is a fine striation (Fig. 6, star). The marginal rim of the ventral disk forms a thin protrusion, which is internal to the cytoplasmic, curved, and tapering extension, the so-called "ventrolateral flange" (Fig. 4) (Friend, 1966).

C. Early signs of nuclear division:

One of the early signs of nuclear division is the appearance of a few, large peripheral blocks of densely packed chromatin fibers (Fig. 7). These dense chromatin blocks have no defined boundary on the inner side and extend as a homogeneous block up to the inner membrane of the nuclear envelope. There is no differentiation at the inner side of the membrane and no structure similar to the nuclear laminae of higher eukaryotes could be defined. The location of these dense masses is always peripheral. A particularly frequent location of one block is at the anterior pole of each nucleus, just below the nuclear pocket in which the basal body of the AF is located (Fig. 7). This basal body (BB1) is seated perpendicular to the nuclear surface, leaving a narrow (about 50 nm deep) space between the body and the nuclear envelope, which is filled with a medium-dense material containing fibrils (Fig. 7).

Among these mature trophozoites there is a significant number of cells—about 10%—that show a nuclear constriction and half-nuclear translocation towards the lower surface of the cell in a bulge or protrusion located at the mid-part of the lower surface (Figs. 8 and 9). This kind of incomplete nuclear division is essentially the same as described below (at the encystation stage) and thus it will be called "downwards type of nuclear constriction".

D. Downwards nuclear constriction:

The serial sections exemplified in Fig. 8 allow a 3D reconstruction (Fig. 9) that shows the following features: A sheet of ventral disk components leaves the main peripheral location of the disk and approaches one of the nuclei, while progressively diminishing the height of the microtubular associated ribbons (Fig. 8). The edge of this sheet near the nucleus becomes tapered down, the periodicity between ribbons becomes narrower and the sheet ends with a height similar to a single microtubular row. Stepwise degrees of nuclear constriction are seen in different cells, but the course of events is better seen in en-

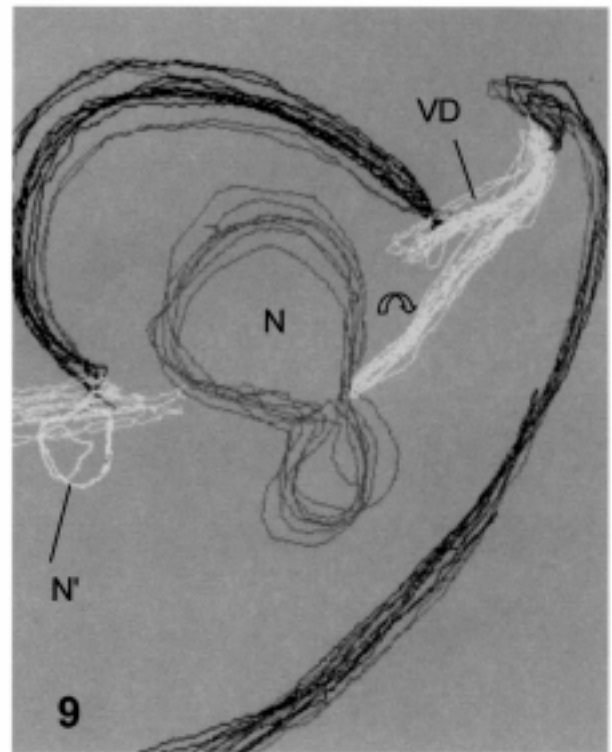
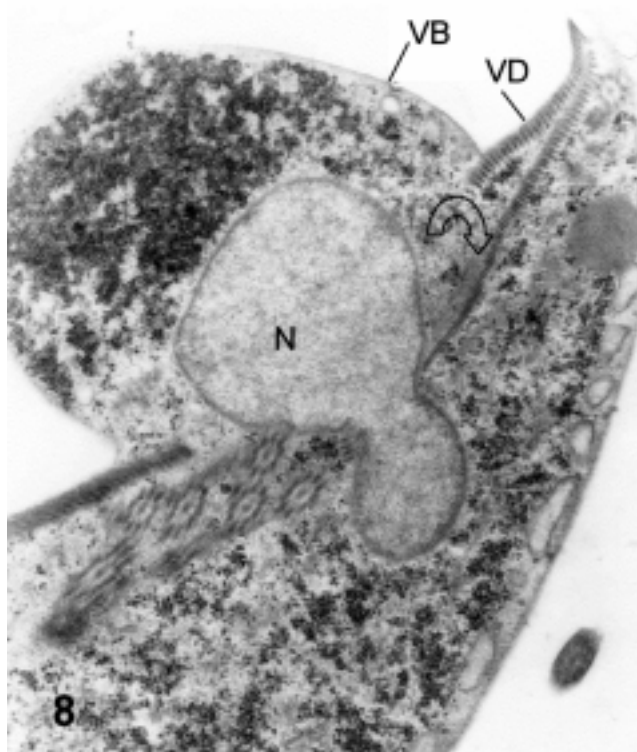
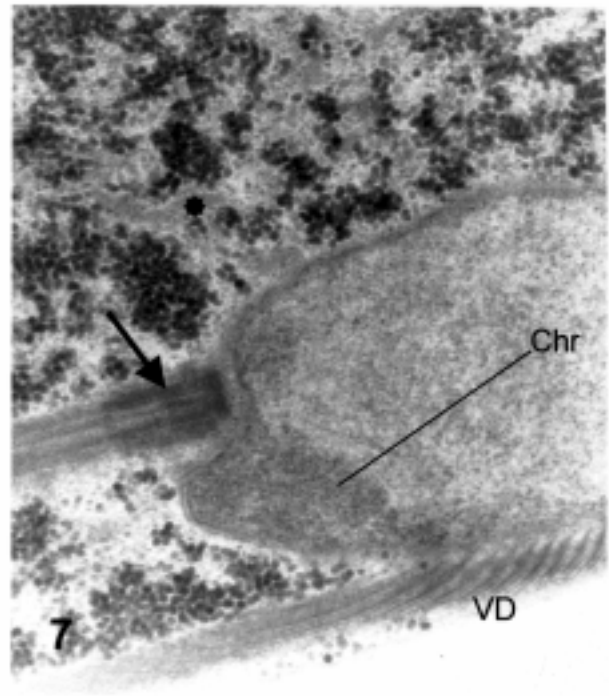
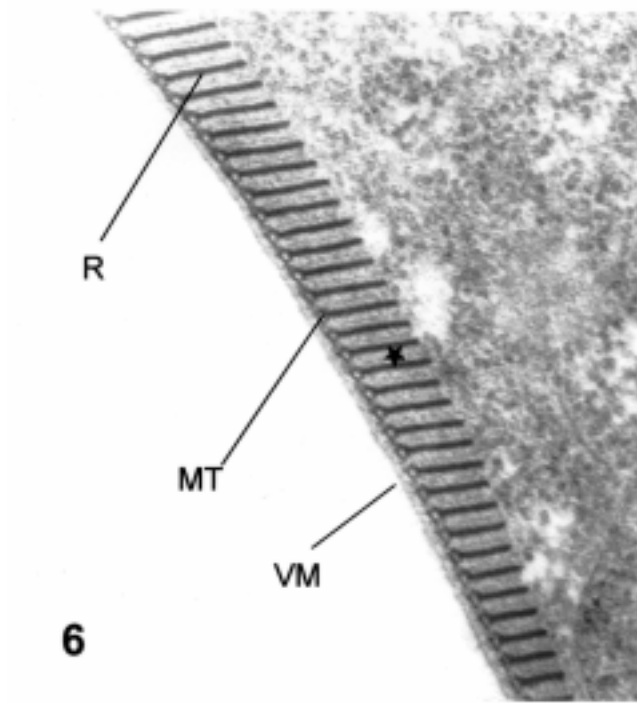


FIGURE 6. Thin cross-section of the ventral disk. VM: ventral membrane. MT: microtubular row. R: ribbons attached to the upper side of the microtubules. A thin intraperiodic line (star) is between each pair of sectioned ribbons. X 60,000.

FIGURE 7. Thin section in a parasagittal plane passing through one nucleus that shows a dense chromatin block (Chr) at the anterior nuclear pole. The arrow shows the anterior basal body sitting on a pocket at the anterior pole of the nucleus. VD: ventral disk microtubules in tangential section. X 32,000.

FIGURE 8. Thin section of a vegetative trophozoite showing the ventral bulging (VB) and the constricted nucleus (N). The constricting sheet derived from the ventral disk is marked by the open, curved arrow. X 18,000.

FIGURE 9. 3-D reconstruction of the nucleus from Fig. 8- The constricting sheet of ventral disk components is marked by the open arrow, and the beginning of the remaining nucleus (N') appears at left.

cysting trophozoites, because the development of the secretory apparatus allows a better sequencing of stages.

The origin and development of this disk-derived sheet is better seen in serial sections in the frontal planes (Fig. 10a-g and 3-D reconstructions in Figs. 10h and 25). Most –and possibly all– the components of the ventral disk originate from the differentiated, anterior pole of the contralateral basal body of a caudal flagellum (Fig. 10a-c). This basal body pole (the “generative”, that is, the non-ciliary one) is covered by four or five parallel, dense layers about 50 nm thick, which have been previously named “dense rods” (Elmendorf *et al.*, 2002). Bundles of tightly packed microtubules with short associated ribbons (Fig. 10a-c and the schematic drawing in Fig. 1B) stem almost perpendicularly from these layers. These bundles, when viewed from the ventral side are curved and follow a clockwise direction (Fig. 10a-g). Along their path, there is a region in which the disk elements are partitioned in two classes: Those having the highest degree of curvature, which are directed towards the constricted nucleus, and those that follow their path towards the caudal region (Figs. 10a-g and 10h). The former make the constricting sheet for the nucleus (NCDE in Fig. 1B), while the latter constitute the main ventral disk. The end of the constricting sheet is plainly visible in Fig. 10h and in semi-thin (0.5 μm thick) sections with light microscopy in many trophozoites. The microtubules forming the sheet seem directed in such a way as to abut perpendicular to the constricted nuclear surface (Fig. 10f-h). However, as shown in the reconstructions, these disk elements end on the cytoplasm, and those closer to the constricted nucleus go tangential to the nuclear envelope (Fig. 8).

While the main mass of the ventral disk components stem from the opposite, caudal basal body, the other caudal basal body originates also a bundle of microtubules and ribbons, with opposite direction to the main one (Fig. 10c-d). However, this bundle is short, and its path has not been followed in 3D reconstructions of early divisional stages.

At the constricted nuclear region the nuclear envelope remains intact (see below). However, at the inner side of the envelope, a small dense mass enclosing circular profiles was seen in some specimens. While the disk-derived sheet is growing, the nucleus adopts a specific dumbbell shape: the posterior part of the nucleus remains at the original horizontal level, while the anterior part of the nucleus traverses the strangled region and goes downwards to the “ventral bulge” (Fig. 8). Some cytoplasmic components, like glycogen, some cisternae, and peripheral vesicles are also pushed into this bulge (Fig. 8).

E. Full nuclear division:

Full separation of each of the parent nuclei into two daughter nuclei is also present among vegetative trophozoites (Figs. 11a-h and 3D reconstruction in Fig 11i). Both the downwards-nuclear constriction and the full nuclear partitioning are non-symmetric respect to the two parent nuclei, as one of the nuclei is the “advanced” one and the other is the “lagging” one.

The full nuclear division, giving 2 pairs of nuclei, is present after a full development of a constricting disk derivative for the “lagging” nucleus”. It seems to be a rapid event due to the low frequency of this stage. This full partition of nuclei leaves each pair of parent-daughter nuclei (1 - 1' and 2 - 2' in Fig. 11) in close proximity, but there are no communicating bridges among them. The chromatin of parent-daughter nuclei has some peripheral denser regions (Fig. 11) but the main chromatin mass remains evenly dispersed. No intranuclear microtubular spindle is observed, and the parallel, close nuclear envelopes in each pair of parent-daughter nuclei (Fig. 11) suggest that nuclear partition is just finished through a nuclear envelope invagination, sealing and separation (Fig. 11a-h). No microtubular bundles that could build as an extranuclear spindle were seen at any stage, with the exception being the microtubules that form part of the two flat derivatives of the ventral disk.

As seen in 3-D reconstructions, the disk derivatives seem to have a further effect on nuclei, besides their constriction. They are located as if they were pushing the nuclear pairs far from each other in a spiral way, that is, both in a lateral and in a dorsal-ventral direction. The plane of parent-daughter nuclear separation is in the dorsal-ventral direction. Cytokinesis is not visible previously to full nuclear partitioning. Basal bodies (8 in the parent cell) are already duplicated when full nuclear partitioning is observed (Fig. 11a-h). The flagella are distributed between the two pairs of parent-daughter nuclei, forming two well-separated groups, which have different orientations (Fig. 11a-h). Rotational-translation symmetry can account for the separate paths of the two flagellar groups (F and F' in Fig. 11a-h).

F. Cytokinesis:

While nuclear partitioning occurs in a dorsal-ventral direction as regards the parent cell, cytokinesis develops while a new ventral disk is developing and the cytoplasmic and nuclear components of the daughter cells are rotating and changing their respective locations

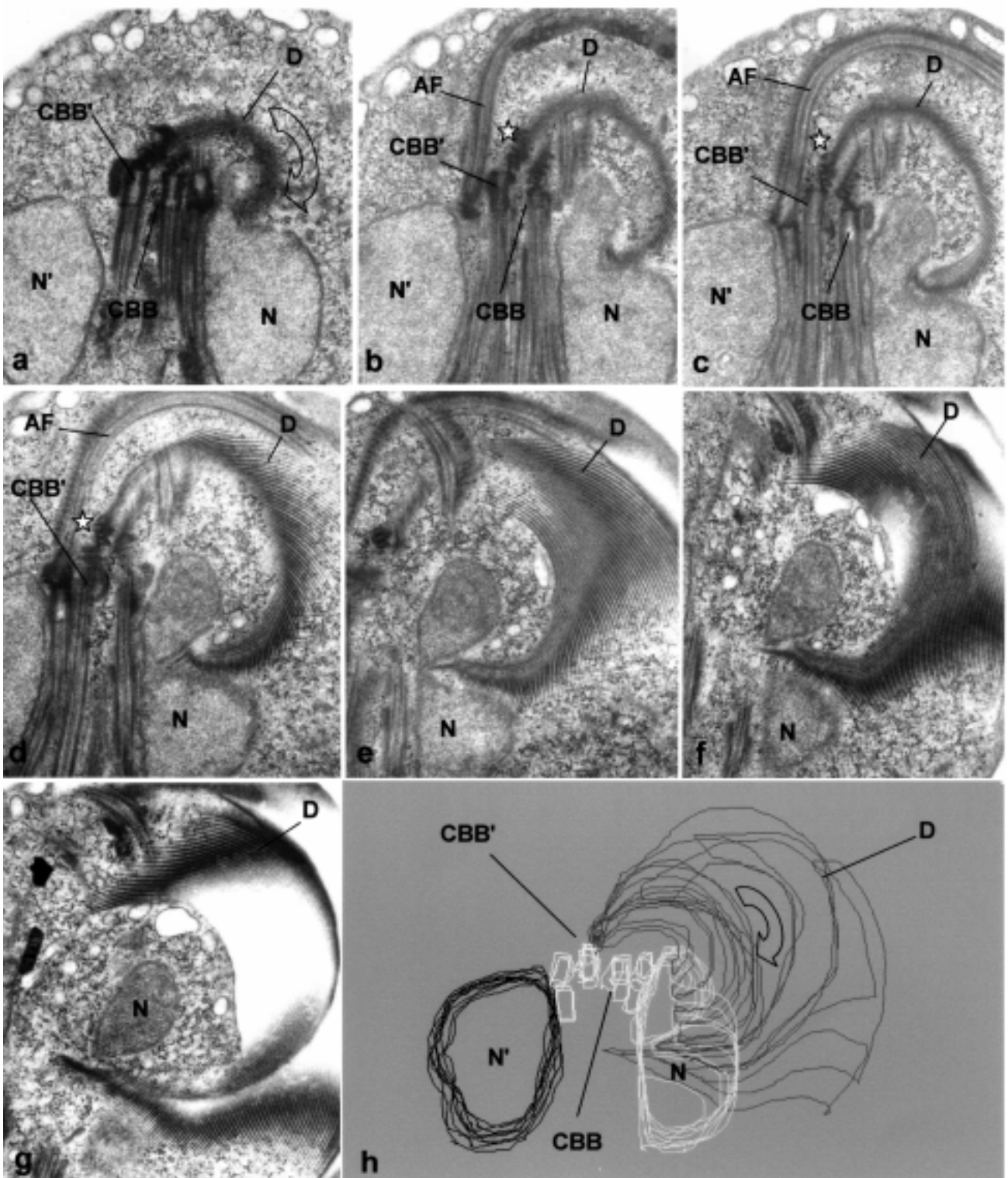


FIGURE 10 a-h. Serial thin sections in a frontal plane showing the path of the constricting sheet of the ventral disk (D). In b-d, the star shows the “dense rods” on the anterior pole of the opposite caudal basal body (CBB’), where the ridges of the ventral disk stem. The constricted nucleus (N) is shown as an apparently divided structure in e-g. CBB, the other caudal basal body. The clock-wise direction of the ventral ridges (open arrow in figure a) shows that it is viewed from the ventral side and that the progression of the serial sections a-g go from the interior towards the surface. The boundary of the constricting sheet is shown as an almost perfect circle in section g, and the constricted nucleus (N) is clearly close to the lower surface. In the 3-D reconstruction (h) the outline of the constricted nucleus (N) is in white, and the other nucleus (N’) in black lines. Additionally, the outlines of all the basal bodies are in white, including the one (CBB’) in which the disk stems. X 14,000.

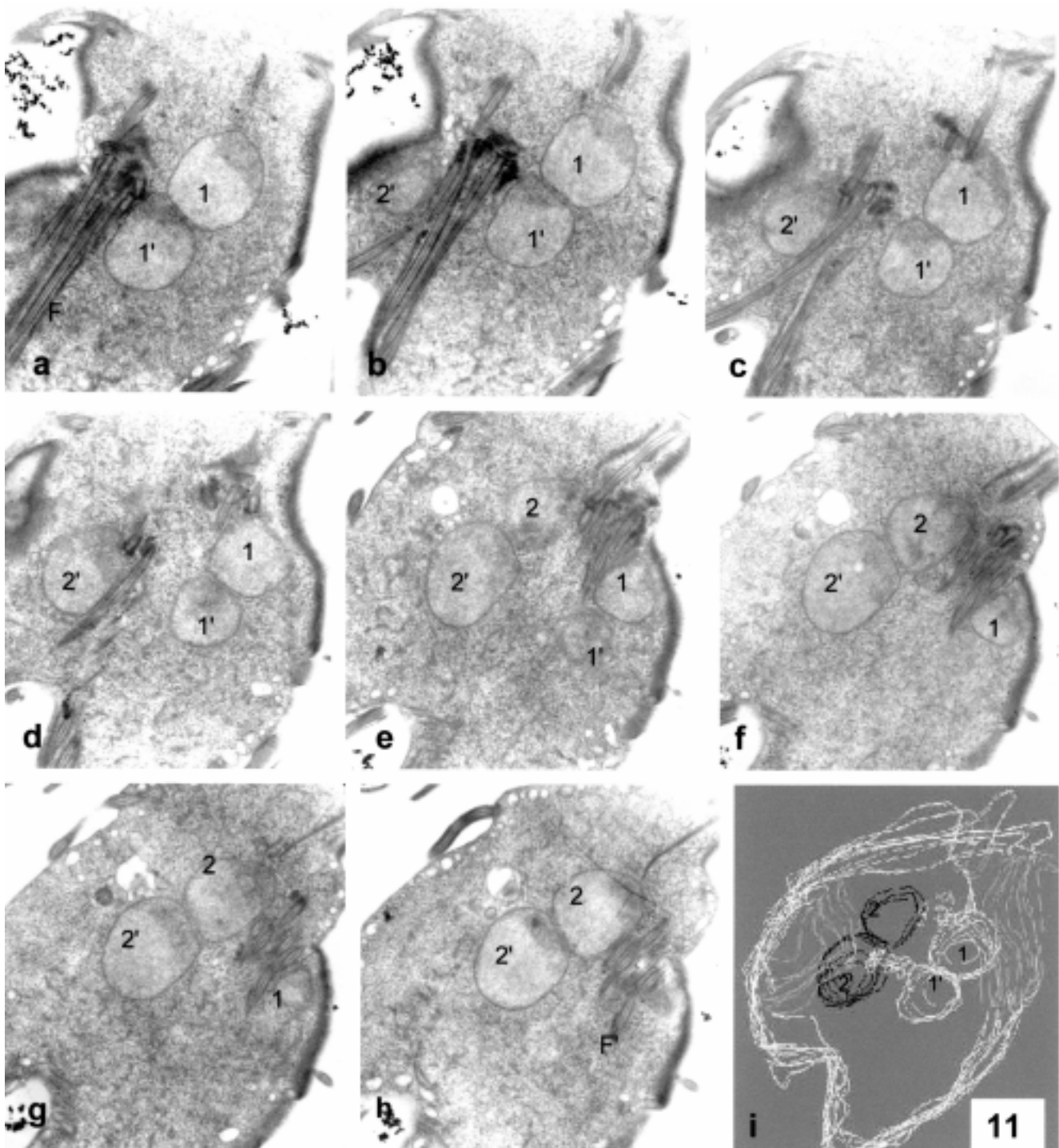
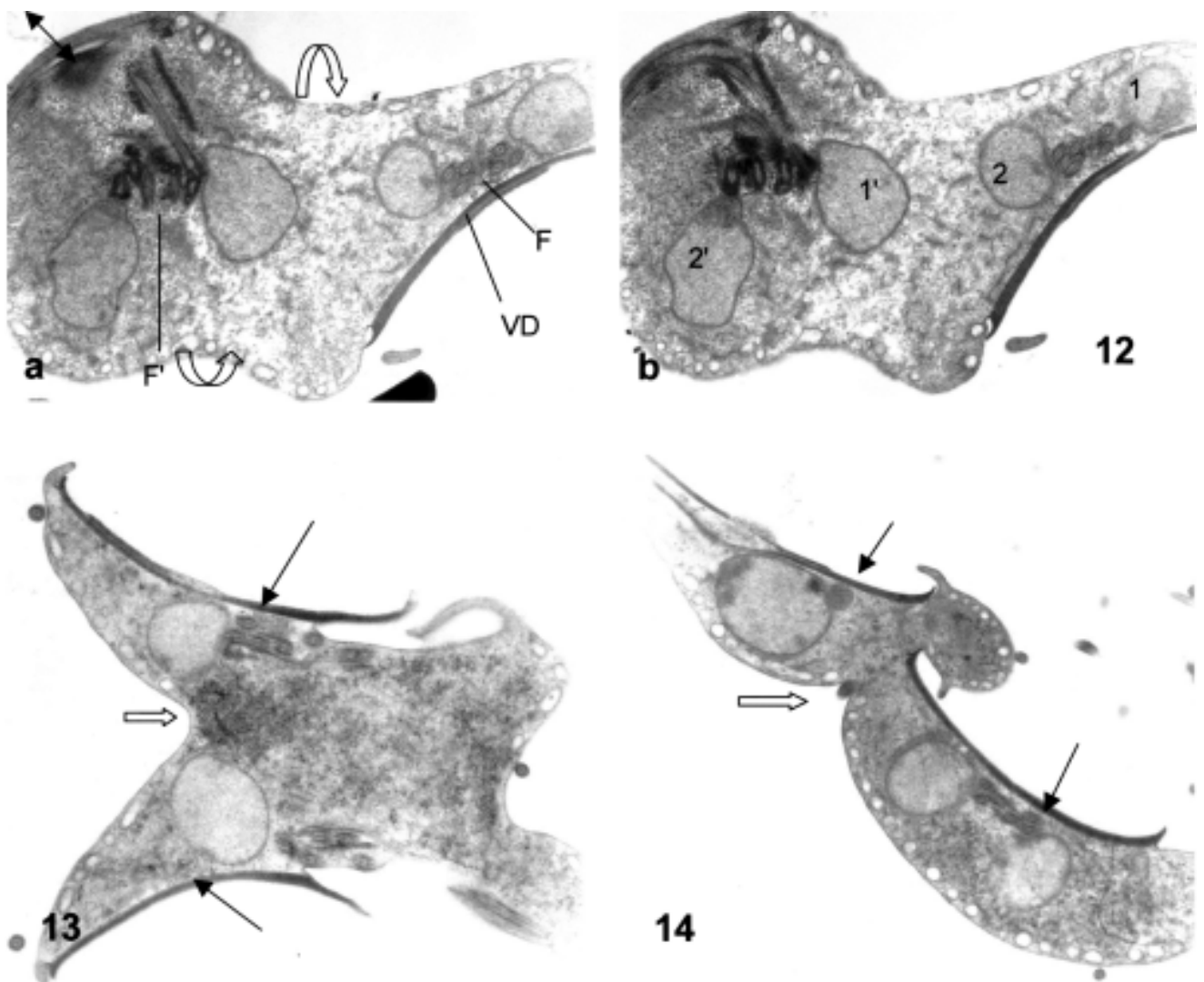


FIGURE 11. Serial thin sections (a-h) and 3D line reconstruction (Fig. i) of a vegetative trophozoite in full nuclear division. The four nuclei are separated in two pairs of parent-daughter nuclei (1 and 1' on one hand and 2 and 2' on the other). Between nuclei 1 and 2 there is a full set of 8 basal bodies and flagella seen in Figs. e-h. Between nuclei 1' and 2' is a second set of basal bodies and their flagella, as seen in Figs. a-c. Nuclei 1 and 2 and their flagella are at the right and upper side and close to the disk on the upper right side of the cell. These elements will form one of the division products. Nuclei 1' and 2' are at the left and lower side, close to an opening disk seen at left in Figs. a-c, and will form the other divisional product. The flagella of this second product are directed left and downwards in Figs. a-c, while the flagella of the former divisional product are directed almost perpendicular to the section plane. There are no connections between parent-daughter nuclei, but their nuclear envelopes are close and parallel to each other. X 6,500.

(Figs. 12A-B and 13). The result of these movements is a general polymorphism in cytokinesis conformations, that gives an early view of dorsal-to-dorsal cytokinesis (Figs. 12 and 13) that in later stages adopts various shapes, as the connecting cytoplasmic bridge becomes thinner and allows different relative positions of the two daughter cells, for instance a side-by-side relationship (Fig. 14).

2. The encystation stage

The pre-cyst stages are characterized by a series of morphological changes in various organelles: A) changes in the adhesive disk, similar to those of the non-encysting trophozoite; B) changes in the secretory system (Golgi, secretory granules, cisternae); C) changes in the surface of the trophozoite, and its overall shape;



FIGURES 12-14. Various aspects of cytokinesis in vegetative trophozoites. In Figs 12a-b the four nuclei (1 and 2 for one cell and 1' and 2' for the other) are well separated and there is a beginning of cytoplasmic constriction for the separation of the cells (open arrows in Fig. 12a). Nuclei 1 and 2 are related to the ventral disk at right (VD in fig. 12a) while nuclei 1' and 2' are related to another disk opening in 12a (double arrow). X 8,300. In Fig. 13 the constricting cytoplasm (open arrow) is separating two daughter cells in a dorsal-dorsal way. The black arrows point to the two ventral disks. In Fig. 14, an advanced stage of cytokinesis shows a lateral joining (open arrow) of daughter cells. Black arrows: ventral disks. X 6,500.

and D) nuclear changes (shape, chromatin, nuclear envelope). These changes occur in a step-wise way, and the reconstruction of the whole process leading to a formed cyst, as described below, involves the observation of many specimens (hundreds).

A. Changes in the ventral disk:

The adhesive disk begins its duplication, and two layers of microtubular rims are now evident. The new one begins just at the place in which the nuclear prominence is becoming strangled between the package of the six central axonemes on one side and the beginning of the new microtubular rim on the other side (Fig. 15). Serial sections allow a 3-dimensional reconstruction of the nuclear evagination, as it becomes clearly a strangled nucleus in way towards the lower cytoplasmic bulge. At some point, half a nucleus is located in the ventral expansion, while the remaining nuclear part remains in the main cytoplasmic body. However, at this point the secretory processes have advanced, the cell becomes surrounded by the newly formed cyst wall, and the whole trophozoite as a unit takes a round shape. The “duplication” of the adhesive disk is actually an intracytoplasmic development of a tapering microtubular-fibrous rim that stretches from the nuclear constriction to the cell periphery. The primitive ventral disk remains as the surface-limiting structure, except at the medial bulge that contains the lower part of the constricted nucleus, glycogen, vacuoles, and the beginning of a cyst wall (see next section). In fact, the first processes of cell wall formation have been observed at this surface of the ventral protrusion.

B. The morphology of secretory processes:

Two very distinct morphological structures accompany the nuclear elongation already described: 1) The upsurge of an elaborate structure resembling the Golgi complex; and 2) the formation of the encystation-specific secretory granules or ESVs (Faubert *et al.*, 1991). A most dramatic phenomenon is the development of a huge stack of flattened, smooth membranous sacs, which pile from 3 to 19 parallel cisternae (Figs. 15 and 16). These stacks form a 2-3 μm -wide cap on one of the two nuclei, which should be easily visible with light microscopy (in fact it corresponds to that described by Lujan *et al.*, 1995, using the Golgi-specific marker NBD-ceramide with fluorescent detection). Typically, the membranous stacks cover the upper part of one nucleus while the other nucleus seems to be involved in the pro-

duction of the secretory (dense, ESV) granules. As seen in Fig. 16, there are several dense large granules, most of them attached to the nuclear envelope of the left nucleus. One granule seems located just inside the nucleus, surrounded by a single membrane, suggesting the involvement of the nuclear envelope in granule formation.

The dense granules are large (about 0.5 μm in diameter) and have a finely granular structure (Fig. 17). Each fine, elementary granule is about 4 nm wide and may form some tubular-like profiles. Both the membranous stacks and the dense granules finally move towards the cell surface.

C. Changes at the surface:

The surface of the ventral protrusion shows the early approach of the flattened sacs (Fig. 18) as well as that of the dense granules. These phenomena are associated with the formation of the cyst wall (see next section). Previous to the mature cyst wall formation, the surface shows a number of thin (2nm) and tortuous filaments all over the cell.

D. Nuclear changes:

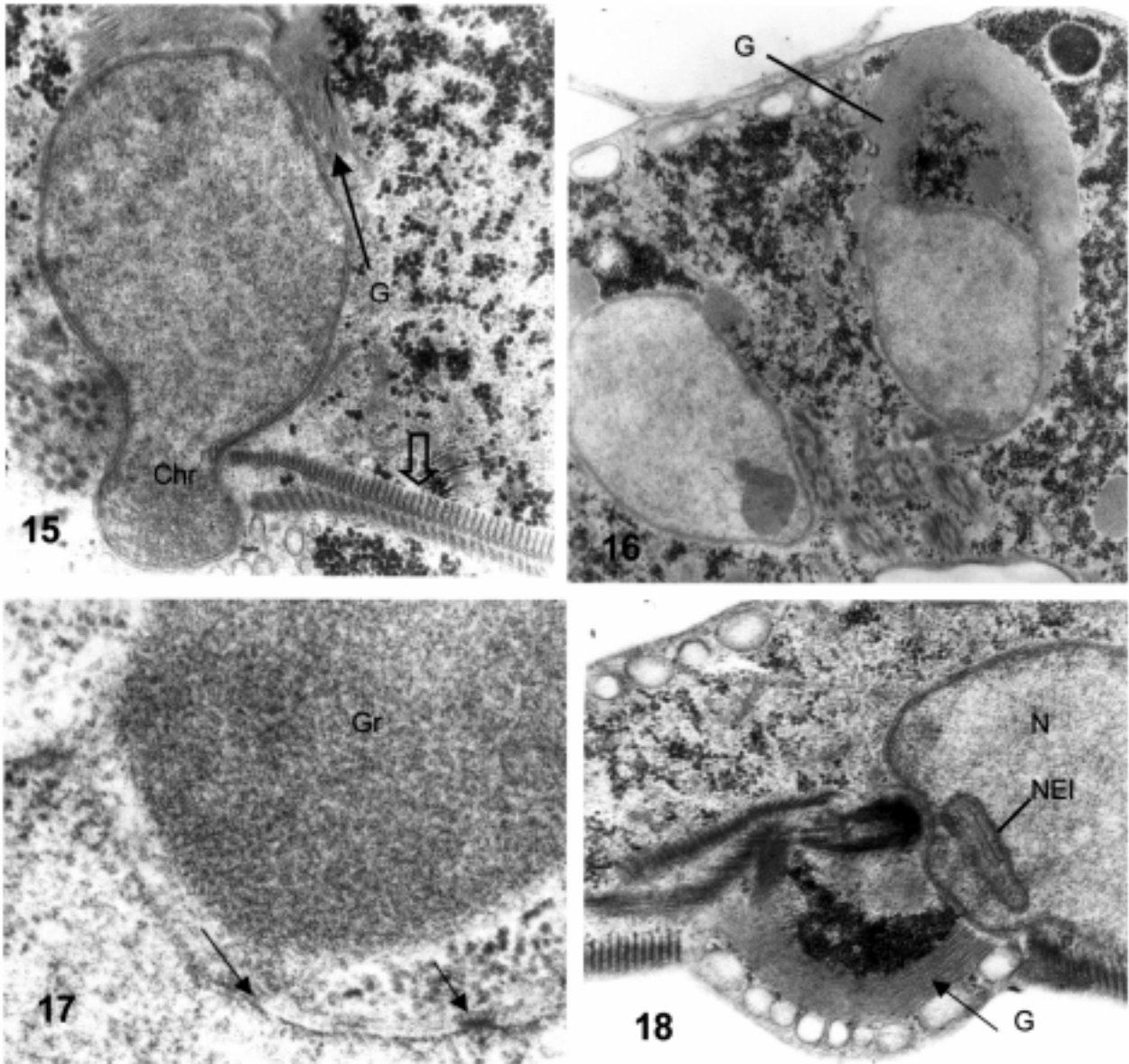
The most striking nuclear changes are the progressive changes in shape and nuclear displacement towards the ventral and frontal side of one of the nuclei (the “advanced” one), which are essentially similar to the nuclear constriction of non-encysting trophozoites. These changes begin at the frontal pole of the nucleus, near the pocket that lodges the basal body of the anterior flagellum (Fig. 7). The chromatin inside the nuclear prominence becomes dense, contrasting with the remaining parts of the nucleus (Fig. 15). In cross-sections it is possible to follow the sequential changes of the nucleus: The nuclear expansion traverses the zone adjacent to the six central flagella and goes down to the ventral protrusion which appears lacking the characteristic microtubular rim of the adhesive disk (Fig. 15). There are also a series of changes in the nuclear envelope of both nuclei. These changes are the earlier ones and may be involved in the later ones. The nuclear envelope develops a sizable amount of nuclear pores (previously absent), especially near the secretory products (Fig. 17). In this figure a specific granule (equivalent to the so-called encystation specific vesicles, ESV) is located on a nuclear depression, in which several pore complexes are observed. The other nuclear envelope process is the development of elaborate invaginations of its two mem-

branes, surrounding some scarce cytoplasmic contents (Fig. 18), and also evaginations of the outer membrane that contain granule-like material (Fig. 16).

3. The fine structure of the cyst and their nuclei

Cysts are oval or round-shaped and completely covered with a thick (0.35 to 0.3 μm) cell wall, which seems

homogeneous at low magnification but shows a filamentous structure at high magnification. Typically, cysts have parallel short and medium-sized fragments of ventral disks dispersed in the medial cytoplasmic region. Axonemes can also be observed immersed in the cytoplasm of the cyst (Fig. 19). The high density of the background is given mainly by packed glycogen granules. The numbers of cross-sectioned cytoplasmic axonemes



FIGURES 15-18. Thin sections of pre-encysting trophozoites. Fig. 15: cross-section showing the constricting disk sheet (open arrow), the dense chromatin at the leading nuclear protrusion (Chr) and the stack of flat cisternae of Golgi (G, black arrow). X 27,000. In Fig. 16 a cross section shows a striking asymmetry between the two nuclei: the right nucleus shows a very large stack of Golgi cisternae (G) while the left nucleus has three specific granules associated to its nuclear envelope, the lower one apparently inside a nuclear invagination. X 15,000. Fig. 17 shows the nuclear envelope and nuclear pores (arrows) at high magnification. A dense granule (Gr) is lying very near to the nucleus. X 70,000. Fig. 18 is a parasagittal section passing through the anterior pole of one nucleus (N) showing a nuclear invagination (NEI). The anterior basal body is at the center. At the lower side there is a ventral bulge having a rim of peripheral vesicles and a large stack of Golgi membranes (arrow, G). X 24,500.

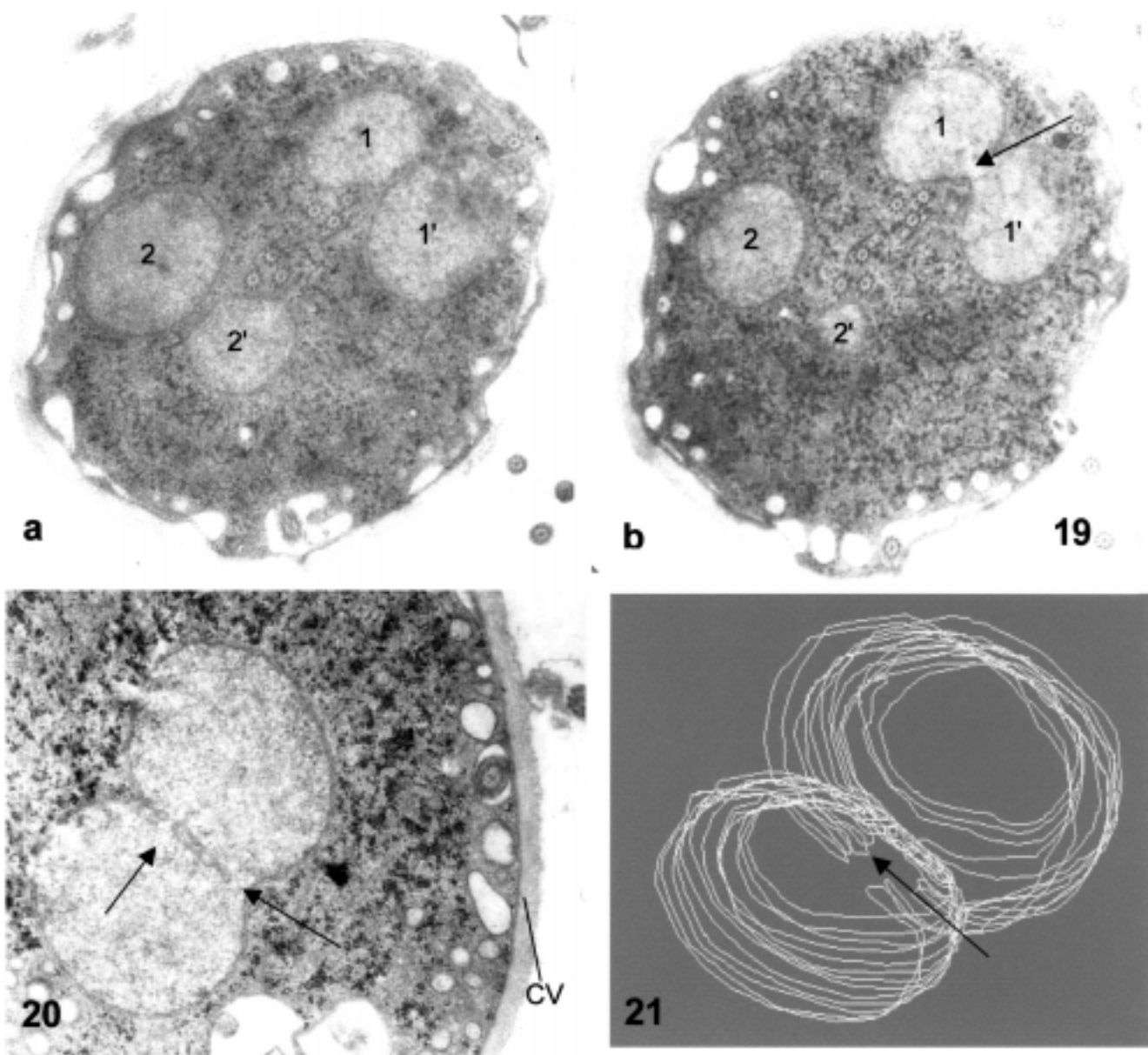
in a full section of a cyst never exceeds 8, and there is no trace of basal body duplication.

Classically, cysts have been considered to harbor four nuclei. A survey of sectioned cysts revealed that actually there are two incompletely divided nuclei (Fig. 19A-B). Nuclei are round and have a dispersed and homogeneous chromatin. While in some sections a full set of four nuclei may appear as true, when serial sec-

tion reconstructions are performed, it is shown that nuclei are connected as pairs. The nuclear connections are relatively narrow ducts on which chromatin seems continuous from one nucleus to the other (Figs. 20 and 21).

4. *The fine intranuclear structure during mitosis*

As the most clear instances of nuclear division are



FIGURES 19-21. Thin sections of cysts and a 3-D reconstruction of the nuclear outlines. The cyst apparently having four nuclei in Fig. 19a (1, 1', 2 and 2') is revealed to have in fact two strangled nuclei in a subsequent section in Fig. 19b. The black arrow in Fig. 19b points to the wide channel communicating 1 and 1'. X 12,000. In Fig. 20 the black arrows point to several channels communicating the parts of a strangled nucleus. X 16,000. In Fig. 21, a 3-D reconstruction of the nuclear outlines shows the nuclear communication (arrow).

seen in trophozoites and during the nuclear extrusion at encystation (see Discussion), a high-magnification series of observations were focused on this fine structure in vegetative trophozoites and encysting cells. No indication of intranuclear microtubular bundles was observed in these instances. However, some kind of oriented, parallel paths of nuclear contents was seen. A particular structure was found at the peripheral clumps of chromatin in the nuclear expansions: A dense core inside the clump, containing tubular-like profiles. However, neither the size, nor the extent and structure of these profiles could agree with microtubular features. True microtubular ribbons, forming small rows of 12–15 microtubules, are often found in the cytoplasm in the medial region containing the axonemes. These microtubules do not attach to the nuclear envelopes, and they do not form part of the median body or the ventral disk, but are independent from them. The “funis”, small rows of microtubules associated with caudal flagella does not attach either at the nuclei.

Discussion

The ordered sequence of events of nuclear division:

The understanding of cell division of *G. lamblia* has been searched for more than a century with little success (reviewed in Filice, 1952, mainly as regards *G. muris*). More recent work has been focused on molecular features of cell division. Based on Feulgen microspectrophotometry, the DNA content of individual trophozoites is 0.144 pg, but the DNA content of cysts is double (0.313 pg of DNA; Erlandsen and Rasch, 1994; Bernander *et al.*, 2001). Thus, one round of DNA replication occurs previous to the mature cyst formation. Confocal microscopy revealed 5 chromosome-like bodies in each of the binucleate trophozoites, in some way suggesting that they represent the 5 electrokaryotype's large bands (Adam, 2001). However, as the data strongly suggest the polyploid status of each nucleus (see Introduction), the cited hypothesis needs further elaboration, as each chromosome-like body cannot simply represent a single chromosome.

In the present results a thorough screening of all stages of the life cycle allowed the discovery of three stages in which nuclear division processes occur: vegetative trophozoites, encysting trophozoites and the excysting stage (unpublished observations). On the other hand, contrary to some stated hypothesis on karyokinesis occurring in cysts (Adams, 2001), the mature cysts do not show any indication of nuclear separation or

nuclear enlargement with formation of peripheral chromatin clumps. Furthermore, the set of basal bodies and axonemes remains as in the trophozoite. The four half-nuclei present in cysts remain connected through well-defined channels filled with chromatin fibers. Thus, the nuclear division that began during encystation featuring nuclear elongation and constriction, with nuclear movement towards the ventral side and the presence of chromatin clumps, remains static and incomplete during the cyst stage.

Some detail of the described processes can be observed with light microscopy. Thus, lobated nuclei, indicative of nuclear constriction by the disk derivative can be observed in spread cells stained with silver nitrate (Fig. 22). The outline of the ventral disk is easily observed with the same technique (Fig. 23) but the inner, constricting sheet is not seen except in semi-thin sections (Fig. 24).

Other stage in which nuclear elongation and strangling occurs is during excystation (Hetsko *et al.*, 1998). However, at this stage the observed phenomena may differ from the vegetative trophozoite (unpublished observations).

Possible mechanisms involved in nuclear deformations and translocation:

The present results show a series of movements involving the whole nucleus and its contents. During nuclear division, the nucleus shows several protrusions that typically contain condensed chromatin. The most evident of these protrusions is the leading frontal one during encystation, but there are other, lateral ones. Similar protrusions are seen at the second divisional round during excystation (unpublished observations). Interestingly, these protrusions are irregular and are not related to the formation of a spindle body as in many other protists, including trypanosomes (Solari, 1980, 1995).

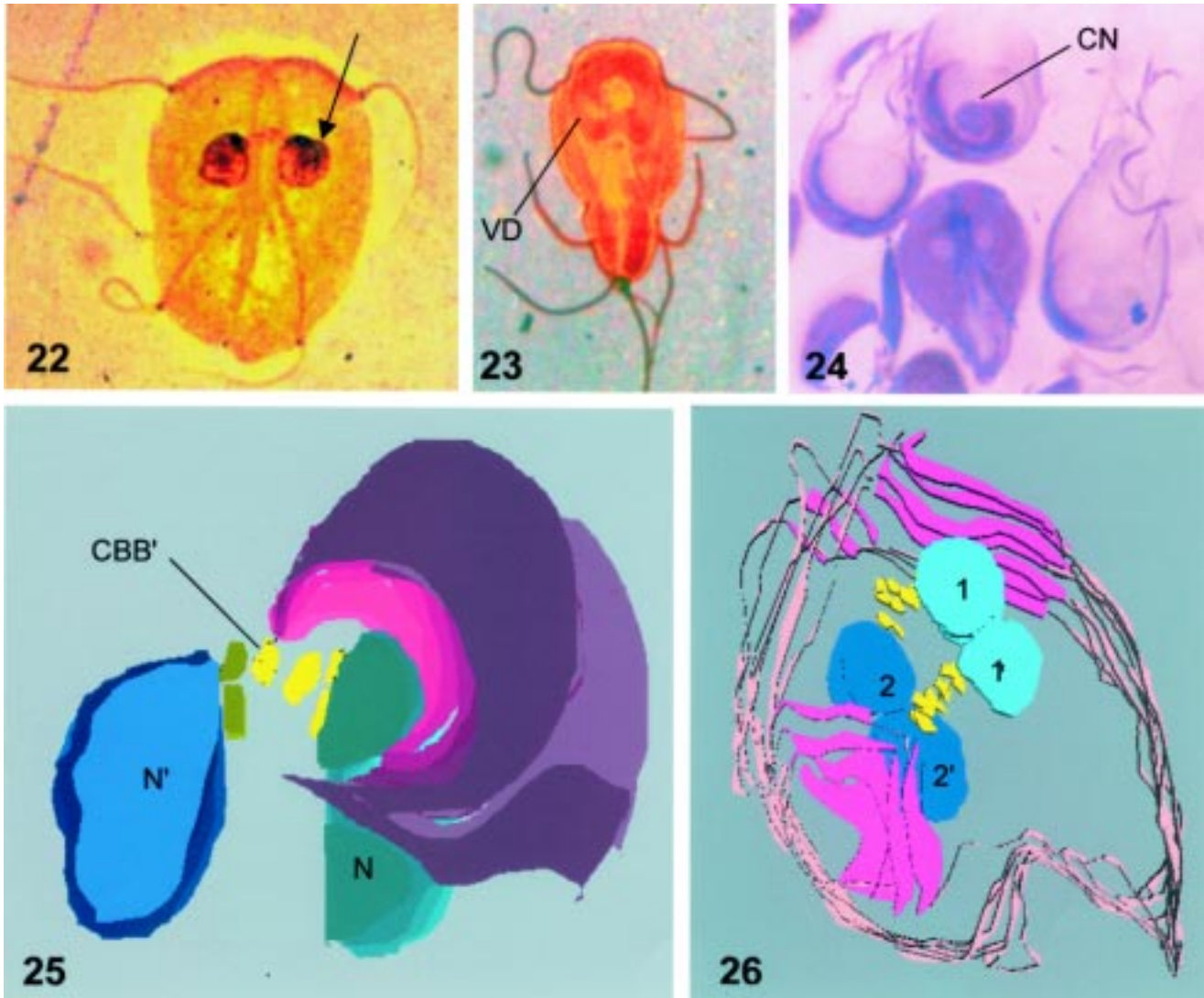
Chromatin condensation in eukaryotes is related to a specific set of proteins, the “condensins” which form part of the large “structural maintenance of chromosomes” (SMC) protein set (Strunnikov, 1998; Hirano, 2000). These proteins are present in *Giardia* (unpublished observations), as it should be expected from an evolutionary viewpoint, because a restricted number of these proteins are already present in prokaryotes (Strunnikov, 1998). It is possible that the nuclear protrusions with condensed chromatin are the so-called “chromosomes” that have often been described with light microscopy.

The translocation of nuclei from their original location to the ventral bulge at the pre-cyst stage is essen-

tially similar in encysting and in vegetative trophozoites. This ventral bulging has been previously described as containing cytoplasmic structures (Lanfredi-Rangel *et al.*, 1999). The downwards-nuclear movement is simultaneous to the nuclear constriction presumably related to the formation of a new microtubular rim or ad-

ditional disk (see Results and model in Fig. 25). The absence of microtubules inside the nuclei poses the question of which mechanisms are responsible for both this movement and the nuclear constriction that occurs during excystation.

The absence of attachments between the nuclear



FIGURES 22-24. Light-microscopical correspondences to fine structure. In Fig. 22, a silver stained, spread protist shows the nuclear indentation (arrow) corresponding to the constricted nuclei in fine structure. X 1,800. In Fig. 23, a silver stained trophozoite shows the doughnut-like shape of the ventral disk (VD), with the central naked region. X 1,500. In Fig. 24, a semi-thin section (0.5 μ thick) stained with alkaline toluidine blue shows the rims of the disk, the pale-blue nuclei and dark-stained basal bodies and flagella at the low center. At the upper center, a sectioned cell shows the spiral path of the disk and a centrally located constricted nucleus (CN). X 1,500.

FIGURE 25. Shows a 3D plane reconstruction of the cell from Fig. 10. The origin of the disk ridges (light and dark magenta tones) is at the caudal basal body marked CBB' (in yellow). The constricted nucleus (green) is tilted towards the observer. The other nucleus (blue) is not indented. The reconstruction shows a ventral view of the cell.

FIGURE 26. Shows a 3D slab reconstruction of the full nuclear division of Fig. 11. The two disks (upper right and lower left) are in magenta and the two sets of basal bodies are in yellow. The parent-daughter pairs are 1-1' (in light blue and 2 and 2' (in deep blue).

envelope and the cytoplasmic microtubular structures suggests that mechanisms other than that based on microtubules (excepted those of ventral disks) are involved in these phenomena.

Actin filaments are known to play important functions during cytokinesis in many eukaryotic cells (Loddish *et al.*, 2000) as well as in cytoplasmic movements like that of pseudopodia (Wang *et al.*, 2003). The presence of actin and actin-associated proteins in *Giardia* has been located at the ventrolateral flange and the ventral disk (Feely *et al.*, 1982) and the protein vinculin has been located in the ventral disk (Narcisi *et al.*, 1994). However, the location of actin and related proteins during the life cycle and especially during the division stages awaits further investigation.

The mechanism of genome partition in Giardia:

It is now evident that *Giardia* has some very peculiar features almost unique among protists (absence of nucleoli, several biochemical traits, etc.). Perhaps one of the most intriguing is the apparent absence of a definite mechanism for the equational partitioning of its genome. There is no definite mitotic apparatus or exonuclear spindle that could account for genome partitioning. *Hexamita* protists, which are phylogenetically close to *Giardia*, have been described to have a "semi-open" type of mitosis (Brugerolle, 1974). Despite suggestions that *Giardia* could have a similar, semi-open mitotic mechanism (Elmendorf *et al.*, 2002) no structure identical to a "polar body" and no polar openings in the nuclear envelope have been demonstrated (see Results). The special association that the basal body of the anterior flagellum has with each of the nuclei might be equated to the role of a "polar body" present in many other protist species (Heath, 1980). However, there is no discontinuity of the nuclear envelope at that place, and thus this possibility remains unproved. A second possibility, as shown in Results, is that expansions derived from the ventral disk are not only responsible for nuclear constriction, but that their microtubules and ridges act as an extranuclear spindle, giving an axis for genome partitioning, which finally occurs by invagination of the nuclear envelope and partitioning of each parent nucleus in a dorsal-ventral direction (see Results and model in Fig. 26). According to the light microscopic observation of Filice (1952) "nucleotomy", that is nuclear partitioning, occurs in a dorsoventral axis, as shown in the present Results. On the other hand, the elaborate chromosome changes described by Filice (1952) have no counterpart in the observed fine structure. As already

mentioned above, the masses of peripheral and densely packed chromatin observed at early stages of nuclear division may correspond to the "chromosomes" described by Filice and by others (Adams, 2001).

The uniqueness of *Giardia* stems from its lack of both intranuclear and cytoplasmic mitotic spindles, and the presence of a ventral disk participating in nuclear constriction, nuclear shaping and axis determination (see Results). The functional role of the ventral disk in attachment has been previously analyzed (Holberton, 1973; reviewed in Elmendorf *et al.*, 2002). The chemical composition of the ventral disk has shown that a particular protein, β -giardin is a component of the disk ribbons, but other components remain undefined (reviewed in Elmendorf *et al.*, 2002).

From a phylogenetic viewpoint, "closed" mitoses, that are those having a permanent nuclear envelope throughout the cell cycle, are considered primitive mitoses (Heath, 1980). Among protists, "closed" mitosis may have a number of variants (Heath, 1980; Raikov, 1994; Solari, 1995; Ribeiro *et al.*, 2002). However, it seems that *Giardia* is the only instance in which a canonical spindle—either intra- or extranuclear—and kinetochores are disposed and replaced by other structures as different as the ventral disk components. Furthermore, in *Giardia* the final nuclear partitioning is dependent on the nuclear envelope (see Results). This fact is in agreement with the hypothesis that primitive divisional mechanisms involve a prominent role of the membranes of the nuclear envelope, as it occurs in prokaryotes with the prominent role of the cytoplasmic membrane (Heath, 1980).

Asexual protists are notoriously less regular in their genome transmission than the sexual ones, as shown by trypanosomes when compared with the sexual *Plasmodia* (Solari, 1995). However, recent data (Yu *et al.*, 2002) suggest that both nuclei of *Giardia* show at least one copy of each of the 5 large chromosomes of electrokaryotypes. The possible ways by which this protist gets an accurate and full amount of their chromosomes, if actual, remains to be investigated.

Acknowledgements

The technical help of Cristina Deparci is thanked. This work is supported by a grant from UBACYT to AJS. HDL received support from the Howard Hughes Medical Institute, CONICET, FONCYT, Fundacion Antorchas and Ministry of Health. AJS and HDL are members of the Carrera del Investigador (CONICET).

References

- Adam RD (2001). *Biology of Giardia lamblia*. Clinical Microbiol Rev. 14: 447-475.
- Bernander R, Palm JE, Svard SG (2001). *Genome ploidy in different stages of the Giardia lamblia life cycle*. Cell Microbiol 3: 55-62.
- Boucher SE, Gillin FD (1990). *Excystation of in vitro-derived Giardia lamblia cysts*. Infect Immun. 58: 3516-22.
- Brugerolle G (1974). *Contribution a l'etude cytologique et phyletique des diplozoaires (Zoomastigophorea, Diplozoa, Danjeard 1910. III. Etude ultrastructurale du genre Hexamita (Dujardin 1838)*. Protistologica 10: 83-90.
- Diamond LS, Harlow DR, Cunnick CC (1978). *A new medium for axenic cultivation of Entamoeba histolytica and other Entamoeba*. Trans R Soc Trop Med Hyg 77: 487-488.
- Elmendorf HG, Dawson SC, McCaffery JM (2002). *The cytoskeleton of Giardia lamblia*. Int J Parasitol (in press).
- Erlandsen SL, Rasch EM (1994). *The DNA content of trophozoites and cysts of Giardia lamblia by microdensitometric quantitation of Feulgen staining and examination by laser scanning confocal microscopy*. J Histochem Cytochem 42: 1413-1416.
- Faubert G, Reiner DS, Gillin FD (1991). *Giardia lamblia: regulation of secretory vesicle formation and loss of ability to reattach during encystation in vitro*. Exp Parasitol 72: 345-354.
- Feely DE, Schollmeyer JV, Erlandsen SL (1982). *Giardia spp.: Distribution of contractile proteins in the attachment organelle*. Exp Parasitol 53: 145-154.
- Filice FP (1952). *Studies on the cytology and life history of a Giardia from the laboratory rat*. Univ Calif Publ Zool. 57: 53-146.
- Friend DS (1966). *The fine structure of Giardia muris*. J Cell Biol. 29: 317-332.
- Ghosh S, Frisardi M, Rogers R, Samuelson J (2001). *How Giardia swim and divide*. Infect Immun 69: 7866-7872.
- Harrison FW, Corliss JO (1991). *Microscopic Anatomy of Invertebrates*. Vol. I, Protozoa. Wiley-Liss, New York, pp. 1-493.
- Heath IB (1980). *Variant mitoses in lower eukaryotes: Indicators of the evolution of mitosis?*. Int Rev Cytol 64: 1-80.
- Hetsko ML, McCaffery JM, Svard SG, Meng TC, Que X, Gillin FD (1998). *Cellular and transcriptional changes during excystation of Giardia lamblia in vitro*. Exp Parasitol 88: 172-183.
- Hirano T (2000). *Chromosome cohesion, condensation and separation*. Annu Rev Biochem 69: 115-144.
- Holberton DV (1973). *Fine structure of the ventral disk apparatus and the mechanisms of attachment in the flagellate Giardia muris*. J Cell Sci. 13: 11-41.
- Lanfredi-Rangel A, Diniz JA, De Souza W (1999). *Presence of a protrusion on the ventral disk of adherent trophozoites of Giardia lamblia*. Parasitol Res 85: 951-955.
- Le Blancq SM, Adam RD (1998). *Structural basis of karyotype heterogeneity in Giardia lamblia*. Mol Biochem Parasitol 97: 199-208.
- Loddish H, Berk A, Zipursky SL, Matsudaira P, Baltimore D, Darnell J (2000). *Molecular Cell Biology*, 4th. edition. W. H. Freeman & Co., New York.
- Lujan HD, Mowatt MR, Conrad JT, Bowers B, Nash TE (1995a). *Identification of a novel Giardia lamblia cyst wall protein with leucine rich repeats. Implications for secretory granule formation and protein assembly into the cyst wall*. J Biol Chem 270: 29307-29313.
- Lujan HD, Marotta A, Mowatt MR, Siaky N, Lippincott-Scwartz J, Nash TE (1995b). *Developmental induction of Golgi structure and function in the primitive eukaryote Giardia lamblia*. J Biol Chem 270: 4612-4618.
- Lujan HD, Mowatt MR, Nash TE (1997). *Mechanism of Giardia lamblia differentiation into cysts*. Microbiol Mol Biol Rev 61: 294-304.
- Lujan HD, Mowatt MR, Nash TE (1998). *The molecular mechanisms of Giardia encystation*. Parasitol Today 14: 446-450.
- Narcisi EM, Paulin JJ, Fechheimer M (1994). *Presence and localization of vinculin in Giardia*. J Parasitol 80: 468-473.
- Nash TE (1992). *Surface antigen variability and variation in Giardia lamblia*. Parasitol Today 8: 229-234.
- Nohynkova E, Draver P, Reischig J, Kulda J (2000). *Localization of gamma-tubulin in interphase and mitotic cells of a unicellular eukaryote, Giardia intestinalis*. Europ J Cell Biol 79: 438-445.
- Raikov IB (1994). *The diversity of forms of mitosis in protozoa: a comparative review*. Europ J Protistol 30: 253-269.
- Ribeiro KC, Pereira-Neves A, Benchimol M (2002). *The mitotic spindle and associated membranes in the closed mitosis of trichomonads*. Biol Cell 94: 157-172.
- Roger AJ, Morrison HG, Sogin ML (1999). *Primary structure and phylogenetic relationships of a malate dehydrogenase gene from Giardia lamblia*. J Mol Evol. 48: 750-755.
- Solari AJ (1980). *The 3-dimensional fine structure of the mitotic spindle in Trypanosoma cruzi*. Chromosoma 78: 239-255.
- Solari AJ (1995). *Mitosis and genome partition in trypanosomes*. Biocell 19: 65-84.
- Solari AJ (1998). *Structural analysis of meiotic chromosomes and synaptonemal complexes in higher vertebrates*. In: Berrios, M., ed., Nuclear structure and function. Methods in Cell Biol. vol 53, pp. 235-256. Academic Press, San Diego.
- Strunnikov AV (1998). *SMC proteins and chromosome structure*. Trends Cell Biol. 8: 454-459.
- Wang H, Oliferenko S, Balasubramanian MK (2003). *Cytokinesis: relative alignment of the cell division apparatus and the mitotic spindle*. Curr Op Cell Biol 15: 82-87.
- Yu LZ, Birky CW, Adam RD (2002). *The two nuclei of Giardia each have complete complete copies of the genome and are partitioned equationally at cytokinesis*. Eukaryot Cell 1: 191-199.